Journal of Sound and Vibration (2001) **246**(2), 199–209
doi:10.1006/jsvi.2000.3500, available online at http://www.idealibrary.com on IDEAL®

AN EXPERIMENTAL INVESTIGATION ON THE ACOUSTIC EXCITATION OF A THIN PLATE BY LOW-SPEED JETS

J. H. Chou, C. H. Ding and S. C. Wu

Department of Engineering Science, National Cheng Kung University, Tainan, Taiwan 701, *Republic of China. E-mail: jungchou@mail.ncku.edu.tw*

(*Received* 17 *April* 2000, *and in final form* 13 *October* 2000)

Experiments were conducted to investigate the acoustic forcing of a thin aluminum plate by low-speed jets. The Mach numbers of the jets were 0·1 and 0·2. The results indicate that the structural response is due to two causes. One is the low-frequency forced excitation of the thin plate due to the leapfrogging interaction of ring vortices. The other one is the natural frequency response at a higher frequency due to turbulent fluctuations in the jet. The former is directionally dependent while the latter is both directionally and position independent.

1. INTRODUCTION

Jets are commonly encountered in engineering applications, e.g., the flow out of an engine exhaust or efflux of pollutants into oceans, rivers or the earth atmosphere. A typical jet in real world could generate noises, especially engine jet noises or air horse jet noises. The noises are annoying and can cause damage to people's health, especially hearing and fatigue problems. The noises may also induce structural vibrations and result in undesirable effects. Because of their practical importance, jets have been studied extensively. For example, Martin [1] gave an extensive description on the heat and mass transfer characteristics of impinging jets. Didden and Ho [2] investigated the unsteady separation behavior of an impinging jet. Rajaratnam [3] summarized the basic features of turbulent jets. In terms of jet noises Morris and Tam [4], Stromburg *et al.* [5], and Troutt and McLaughlin [6] suggested that vortex pairing is a noise generation mechanism. Vortex pairing is a process typically occurring in two-dimensional vortices. In an axisymmetric jet where a vortex is in the form of a ring, the leapfrogging phenomenon is the counterpart of vortex pairing in two-dimensional vortices. In this regard, Gurzhii and Meleshko [7] showed that vortices generated the largest sound field during the process of one vortex ring passing through another one. This passing process is usually referred to as leapfrogging. On the other hand, Hussain [8] pointed out that vortex pairing is not likely to be observed unless the flow is stable and laminar. Zaman [9] and Bridges and Hussain [10] gave the same conclusions and raised doubts about the role of vortex pairing in turbulent jet noises, especially in practical situations where the potential core of a jet is not evident. There seems to be a need to address the differences among these studies. Furthermore, as pointed out by Verma and Rathakrishnan [11] and Brassard *et al.* [12], the nozzle geometry has great influence on the jet noises.

Most practical jets are turbulent. Turbulent flows are noisy. Bies *et al.* [13] investigated the aerodynamic noise generated by a stationary body in a turbulent air stream. Their result indicated that a bluff body could be a powerful noise source. This is expected since vortices

0022-460X/01/370199 + 11 $35.00/0

tend to prevail with bluff bodies. For jet noise–structural interactions, Davis and Pan [14] investigated the effect of a rigid plate on the noise generated by a turbulent circular jet by placing the plate on the axis of the jet. They compared the sound pressure level measured with existing sound theories. Fanno *et al.* [15] studied the forcing of a panel structure by a nearly sonic jet. In the latter two studies, the structures were all parallel to the jet axis. In this study, the acoustic forcing of a panel by jets are studied by placing the plate at various angles to the jet axis.

2. EXPERIMENTAL METHODS

A circular nozzle is used to create the jet flow-field. A schematic diagram of the nozzle is shown in Figure 1. The nozzle is made of stainless steel and consists of a diffusing section, a settling section and a contracting section. The diffusing angle is 3·5° so that flow separation can be avoided. Three screens are installed in the nozzle, one in the diffusing section and two in the settling section. In addition to screens, a honeycomb is also installed in the settling section. A fifth order polynomial is used to create the shape of the contracting section. The contraction ratio is 7 so that a good-quality jet flow can be obtained.

The co-ordinate system adopted in this study is depicted in Figure 2. It should be noted that the symbols x and D represent the axial distance of the jet and the nozzle exit diameter, respectively.

The thin aluminum plate has a size of 500 mm (length) × 400 mm (width) × 2 mm (thickness). Three inclination angles are examined, i.e., 0, 45 and 90° respectively. For the 0° inclination case, the thin plate is installed horizontally with its bottom surface at a distance of 10D from the centerline of the jet. For 45 and 90° cases, the central point on the bottom surface of the thin plate is right on the axis of the jet. A schematic diagram of the three inclination cases is shown in Figure 2. During the experiments, the 500 mm side of the thin plate is inserted and rigidly tightened by six equally spaced screws into a plate support. The plate support is outside the jet to reduce flow disturbances. On the plate, an accelerator is attached to the center of the plate to measure the dynamic response of the plate.

A Pitot tube is used to measure the velocity distribution. A constant temperature hot-wire anemometer is used to measure the turbulence characteristics of the jet. The wire has a length-to-diameter ratio of 250. The over heat ratio is 1·6. A Rion's sound meter, with embedded microphone, is used to measure sound pressure level of the jet. The meter can be a noise source [13]. In this study, the meter is brought into the jet with its axis parallel to the jet axis. Thus, vortex shedding from the wake of the meter and the associated noises can be

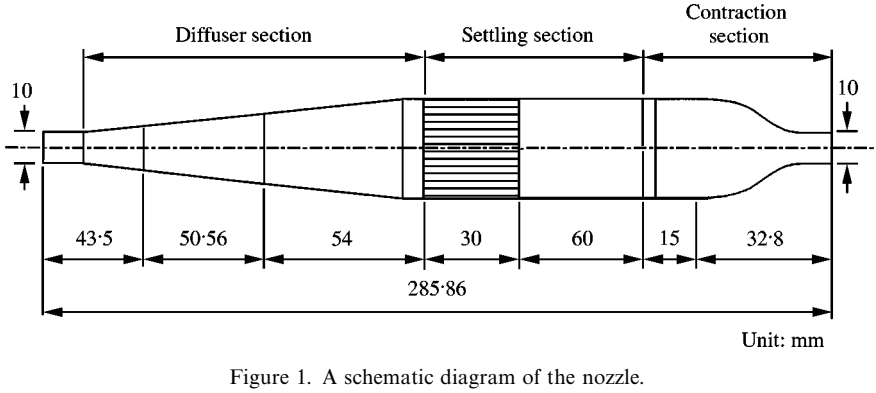

Figure 1. A schematic diagram of the nozzle.

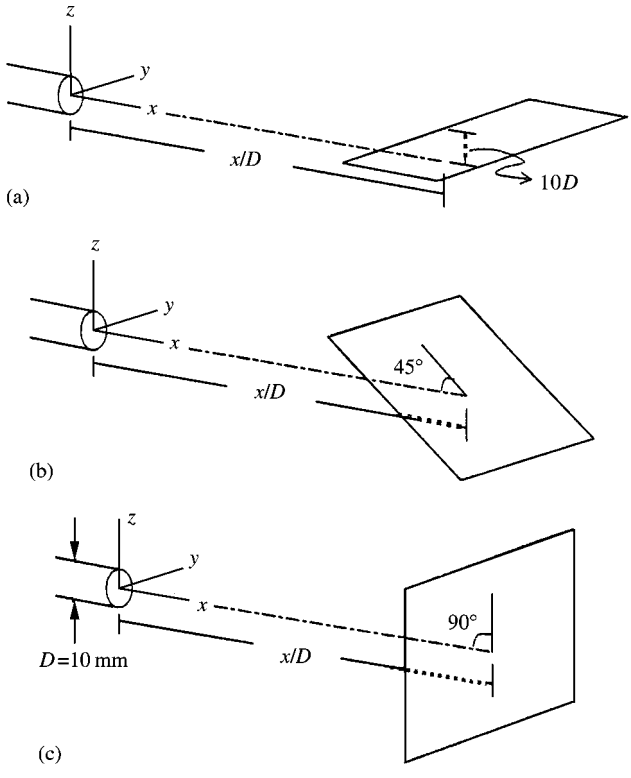

Figure 2. The co-ordinate system and the thin plate configuration: (a) 0° inclination angle; (b) 45° inclination angle; (c) 90° inclination angle.

reduced. Fast Fourier transforms are used to extract essential features of the turbulence signals and the noise-induced dynamic response of the thin aluminum plate. Two Mach numbers, 0·1 and 0·2, are investigated. The corresponding Reynolds numbers are 25 000 and 50 000 respectively. Experiments are conducted typically from midnight to about 4:00 a.m. in an open site of $30\,\text{m} \times 35\,\text{m}$ horizontal area. Noise reflection from the floor is unavoidable for this type of facility. However, the jet axis is about $160D$ above the floor and measurements are made only to $x/D = 50$. Thus, background noise and noise reflection from the environment can be reduced to obtain meaningful results.

3. RESULTS AND DISCUSSION

Typical mean velocity distributions of the turbulent circular jet are shown in Figure 3 where the Mach number is 0·1 and 0·2 in Figures 3(a) and (b) respectively. The symbols U and U_c represent the mean axial and centerline velocity of the jet respectively. It can be seen that the potential core ends at about either $5D$ or $10D$, depending on the Mach numbers. The potential core of the Mach number 0·2 case is twice that of the Mach number 0·1 case. For locations $x/D \geqslant 5$ or $x/D \geqslant 10$, the velocity distributions are symmetric bell shapes and exhibit turbulent features. The potential core for both cases is either equal or larger than the conventional value of $5D$, e.g., reference [16]. This observation implies that the nozzle of the present study is well designed and has a lower disturbance level at higher Mach number 0·2.

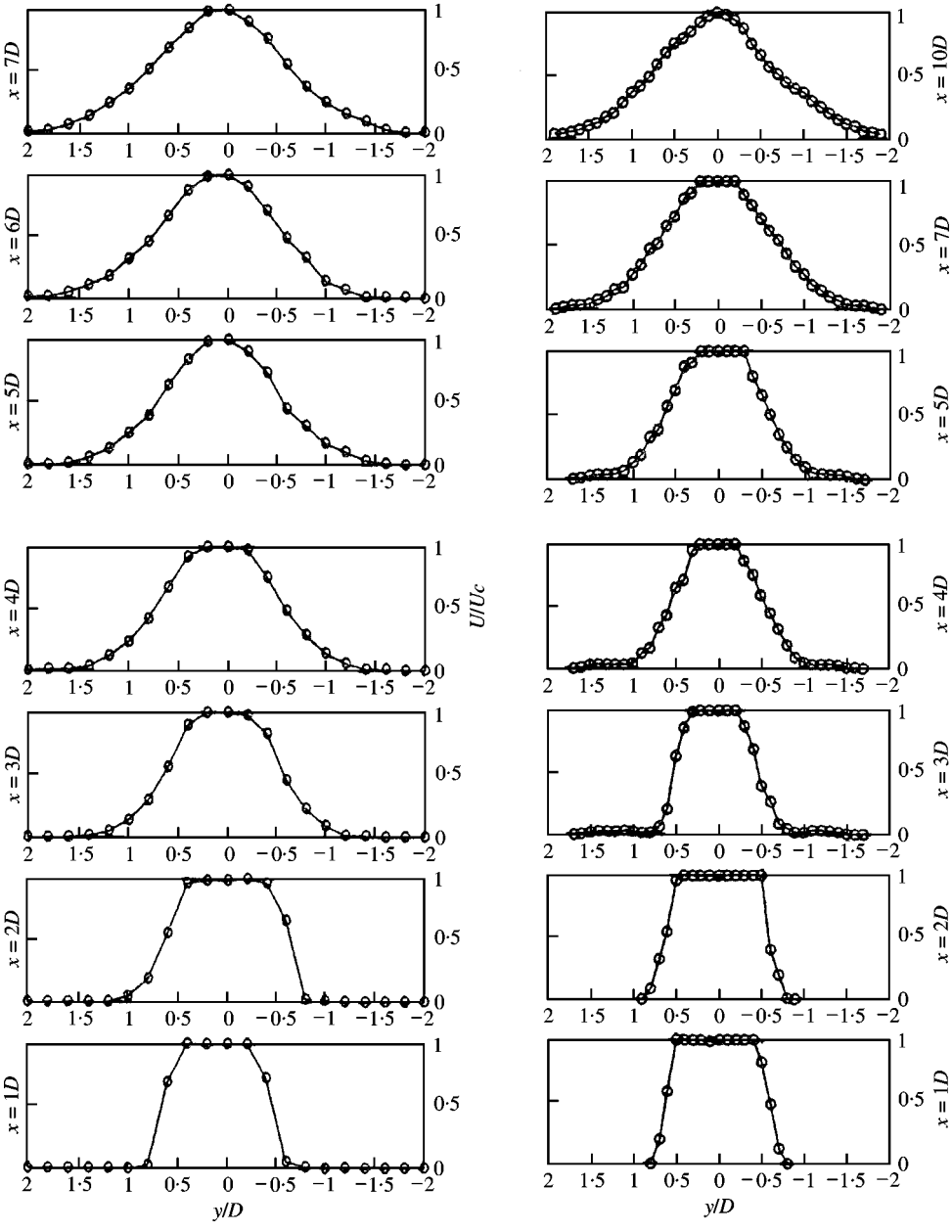

Figure 3. Measured mean velocity distributions of the turbulent circular jet. (a) Mean velocity distributions (Mach number = 0·1); (b) mean velocity distribution (Mach number = 0·2).

The characteristics frequency of turbulent velocity fluctuations of the jet is shown in Figure 4 for Mach number 0·2. The frequency distribution is obtained from FFT of the hot wire turbulence signals measured along the centerline of the jet. It should be noted that frequency distributions exhibit two distinct features; namely, a low-frequency (with side band) part and a discrete high-frequency (with its harmonics) part. Thus, the features are expressed in terms of Strouhal numbers for these two types of frequencies. The Strouhal number is defined as $f U_c/D$. The symbols f, U_c and D represent the characteristic frequency,

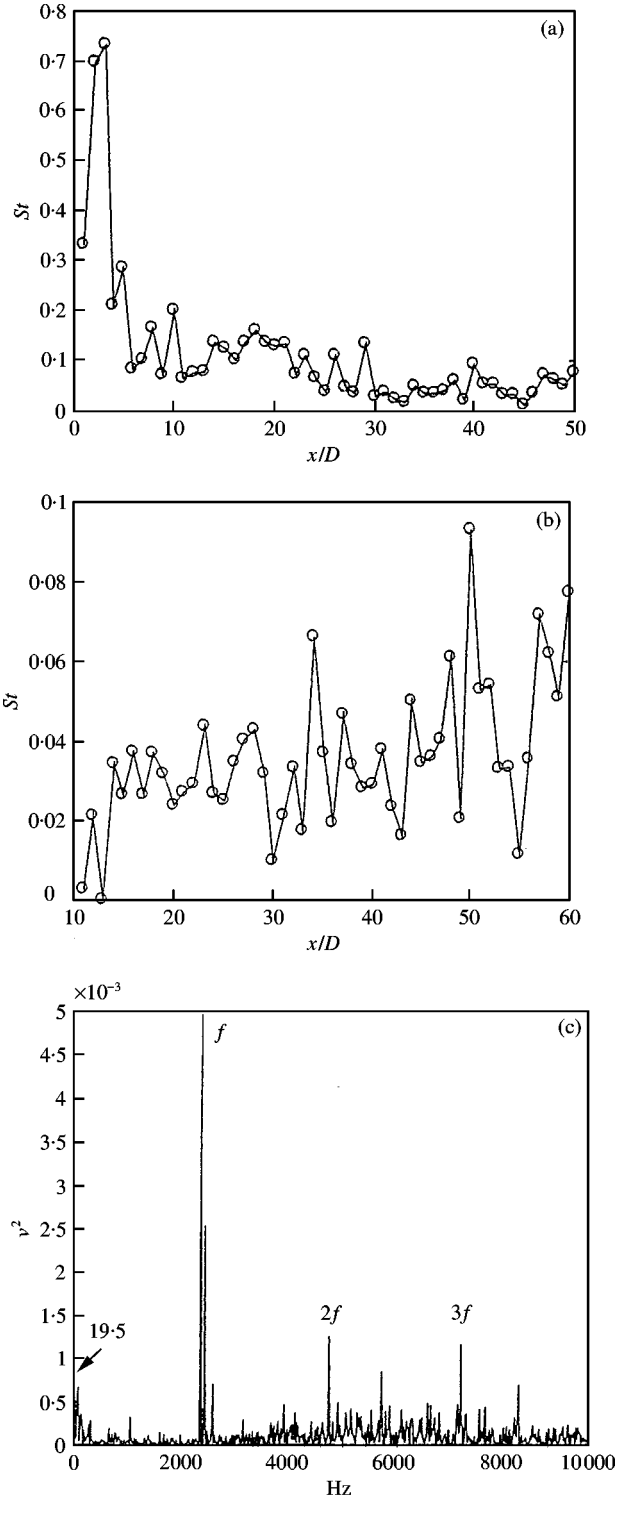

Figure 4. The frequency contents of turbulent fluctuations of the jet, Mach number = 0·2. (a) High-frequency part; (b) low-frequency part; (c) the original frequency distribution at $x/D = 1$.

the mean local centerline velocity and the nozzle exit diameter respectively. It can be seen from Figure 4(a) that, for the high-frequency content, the Strouhal number increases sharply from $0 \leqslant x/D \leqslant 5$, reaching a peak value of slightly greater than 0·7. The Strouhal number then decreases, again sharply, from $5 \leqslant x/D \leqslant 10$. For $x/D \geqslant 10$, the characteristic frequency oscillates around a fairly constant value of approximately less than 0·1. On the other hand, the low-frequency content, shown in Figure 4(b), increases drastically from $0 \leqslant x/D \leqslant 5$ and remains a nearly constant value of about 0·033 for $5 < x/D < 20$. For $x/D > 20$, the Strouhal number increases slightly, but the variation is quite large. As mentioned previously, the potential core for Mach number 0·2 case is about 10. Thus, the hot wire signals obtained for $0 \leqslant x/D \leqslant 10$ essentially represent flow disturbances in a potential core. In order to gain a deeper understanding of the frequency characteristics, the original frequency spectra are closely examined. The frequency distribution at $x/D = 1$ is shown in Figure 4(c) as a typical example. The notation V^2 denotes volt-square, representing the energy level of the fluctuation at each frequency. The original spectrum indicates that there are three kinds of fluctuations at this location. The first one is associated to the frequency of random signals. It is a wide band noise with a very low energy level, indicating the well-designed nature of the nozzle. The second one is a discrete high frequency denoted by f and its harmonics. The value of f is about 2441 Hz with a corresponding Strouhal number of 0·33. The value is consistent with that of reference [6] and represents the characteristic frequency of the shear layer instability that leads to the generation of ring vortices. In other words, the high-frequency part of the spectrum is due to shear layer instability and is the dominated frequency component at this location. The third one is a low-frequency content centered around 19·5 Hz. There are two possible sources that could result in a low-frequency structure. One is the turbulent structure of the flow. The other is the leapfrogging interaction of ring vortices. In the potential core, there is no turbulence, except the random noise just mentioned. Thus, the low frequency of 19·5 Hz is most likely related to the large-scale structure associated with the leapfrogging interaction of vortex rings. Therefore, the sharp decrease of high frequency from $x/D = 5$ and the drastic increase of low frequency up to $x/D = 5$, shown in Figures 4(a) and (b), respectively, indicate that vortex rings are being formed in the region of $0 < x/D < 5$. The leap-frog interaction between vortex rings takes place in the neighborhood of $x/D = 5$. For smaller x/D values, the energy is dominated by the shear layer instability. However, at $x/D \fallingdotseq 10$, energy contained in the harmonics (about 176 Hz) of low-frequency component is the dominated one. As the axial distance x increases farther from $10D$, the high peaks in the spectrum corresponding to the shear layer instability diminishes quickly. Turbulence signals become the dominated feature of the spectrum. However, on top of the turbulence spectrum, the harmonics of the low-frequency component still persists even to downstream locations as far as $x/D = 50$. In other words, the low-frequency structure tends to prevail in most of the flow-field. This is reasonable since shear layer instability exists only in the neighborhood of the potential core and damps out quickly. On the other hand, the low-frequency component is observed over the range of x/D being studied. Since the low-frequency source is near $x/D = 5$, this implies that a low-frequency effect is detected in both upstream and downstream directions.

The noise level measured by the sound meter along the centerline of the jet is shown in Figure 5. It can be seen that the noise level increases initially, reaches its maximum value in the neighborhood of $x/D = 5$, and then decreases as x/D increases further. The decrease rate from its peak value is faster for the Mach number 0·1 case than for the Mach number 0·2 case. This is expected since the potential core for the former case is shorter than the latter one. It can also be observed that higher Mach number causes higher noise level, consistent with daily experience. In order to get a deeper insight into the noise distribution, the

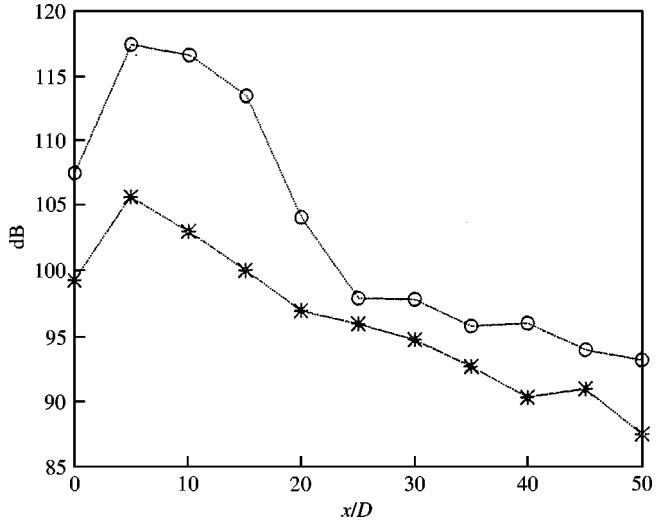

Figure 5. The noise level along the centerline of the jet (circle for Mach number = 0·2).

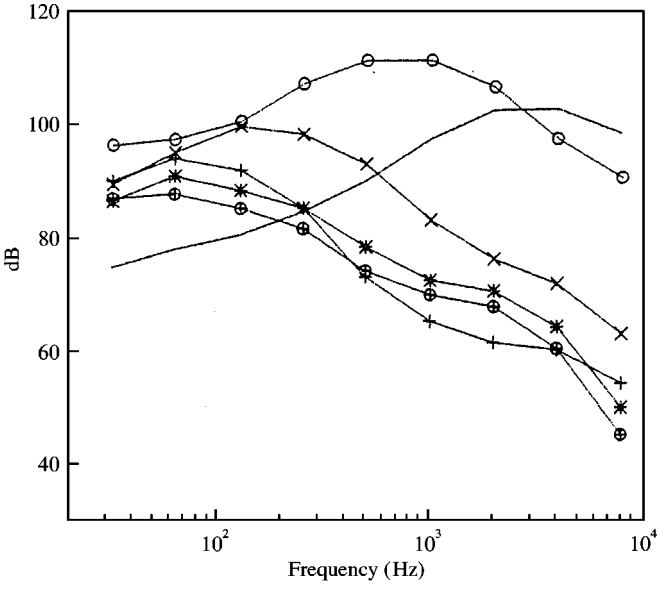

Figure 6. The frequency content of the noise along the centerline of the jet, Mach number = 0·2: $x/D = 0$; ——, $M = 0{\cdot}2$; $x/D = 10$; - -○- -; $x/D = 20$; - - × - -, $x/D = 30$; - - + - -, $x/D = 40$; - - ⋇ - -, $x/D = 50$; - - ⊕ - -.

frequency content of the noise along the centerline is examined. The distribution for the Mach number 0·2 case is shown in Figure 6. It can be seen, over the frequency range deduced, that the peak noise level increases for x/D from 0 to 10 and then decreases for further larger values of x/D. Furthermore, high-frequency contents dominate the noise field in the region close to the nozzle exit. Then the dominating frequency shifts to lower frequencies as x/D increases further. This is consistent with the previous description of the characteristics of the jet flow-field. It is also interesting to note that the trend of the noise frequency distribution is similar for farfield locations with $x/D \geqslant 20$, most likely due to the similarity of turbulence structures. It should be mentioned also that the trend for the Mach

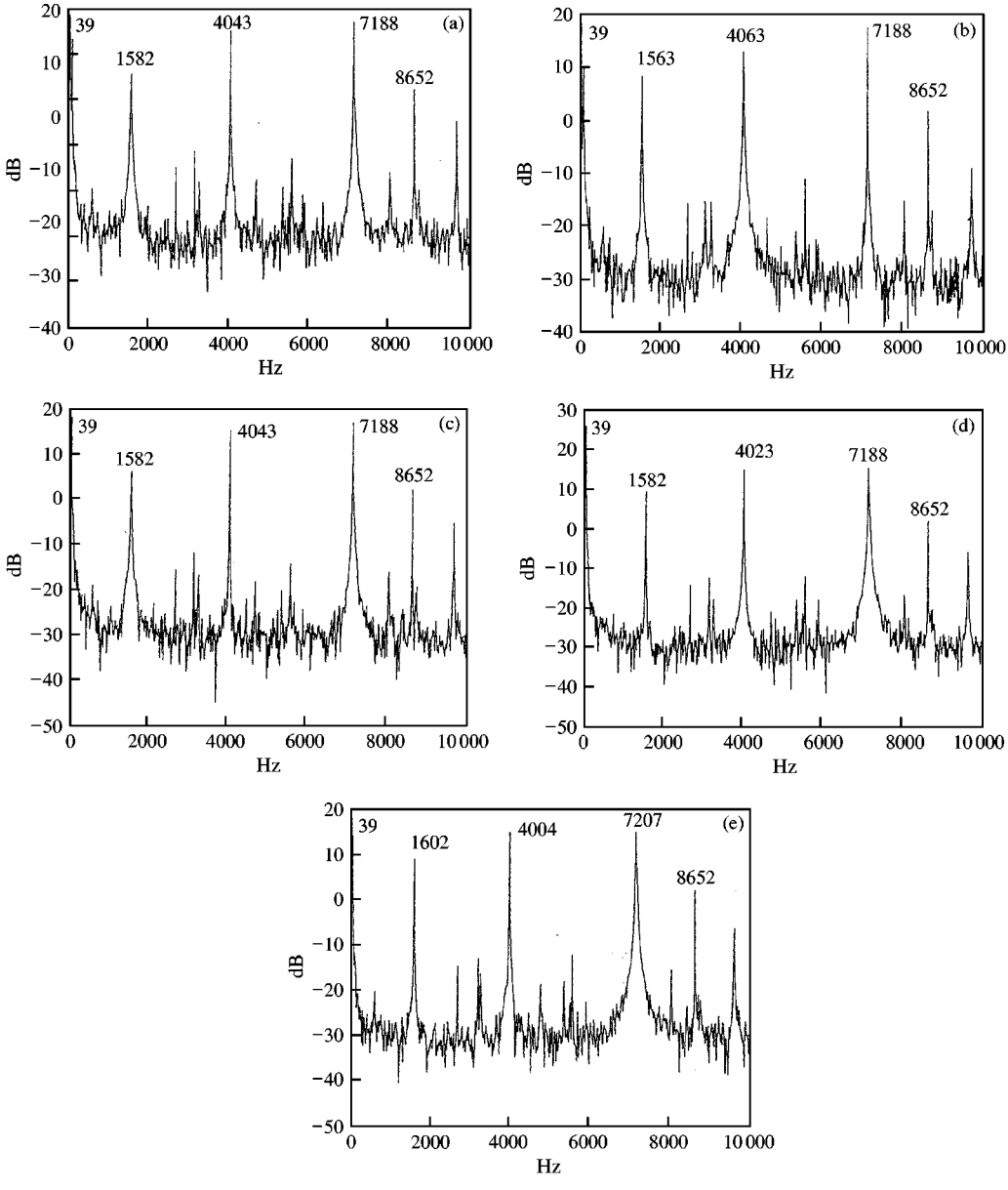

Figure 7. The response of the thin plate to the jet, Mach number = 0·2. (a) $x/D = 10$; (b) $x/D = 20$; (c) $x/D = 30$; (d) $x/D = 40$; (e) $x/D = 50$.

number 0·1 case is similar, except that the noise level at the corresponding frequency is lower.

With this background noise information, the effect of the jet noise on a thin aluminum plate was investigated. The results of Mach number 0·2 case are presented since the potential core is longer and the noise level is higher in this situation. Data of five axial locations are presented in Figures 7(a)–(e) for $x/D = 10$, 20, 30, 40 and 50 respectively. The inclination angle of the thin plate is 0°. As can be seen from Figure 7(a), the spectral response of the plate to the jet noise field at $x/D = 10$ shows discrete peaks. The first four dominated frequencies are 39, 1582, 4043 and 7188 Hz respectively. They are clarified as

TABLE 1

The low-frequency response of the thin plate

θ \ $x\backslash D$	10	20	30	40	50
0°	39 Hz	39 Hz	39 Hz	39 Hz	39 Hz
45°	78 Hz	137 Hz	78 Hz	78 Hz	78 Hz
90°	39 Hz	195 Hz	78 Hz	78 Hz	78 Hz

low- and high-frequency part of the spectrum content. The low-frequency part is 39 Hz and the rest are high-frequency parts. To obtain some insight into the high-frequency content of the spectrum, the Rayleigh method [17] is used to estimate the natural frequency of the plate. The first three modes of its natural frequencies computed are 1612, 4036 and 6753 Hz respectively. The computed results are close to the measured high-frequency ones. At other x/D locations downstream, given in Figures 7(b)–(e), the low frequency at each x/D remains at the value of 39 Hz. The frequencies of the first high-frequency mode measured are 1563, 1582, 1582 and 1602 Hz for $x/D = 20$, 30, 40, 50 respectively. Even though there are variations in the measured values, they are close to the computed natural frequency of 1612 Hz. The corresponding measured second mode frequencies are 4063, 4043, 4023 and 4004 Hz, also close to the computed value of 4036 Hz. Similar observations can be obtained for the third mode. In other words, for the range of x/D investigated, the response of the plate to the jet noise field is independent of the plate location. As described previously, turbulence is the key feature of the jet flow for $x/D \geqslant 10$ for the Mach number 0·2 case. It is also well known that turbulence has a wide band spectrum in its energy content [18]. Thus, the high-frequency response of the plate at corresponding natural frequencies is due to turbulence excitations. On the other hand, the low-frequency response of the plate is due to the forced vibration of the large-scale structure of the flow which originates from the leap-frog interaction of ring vortices.

For the inclination angles of 45 and 90°, the response of the plate exhibits similar behaviors to those of 0°. The response of the plate can also be grouped into two parts; namely, the low- and the high-frequency parts. The high-frequency parts are also the natural frequency response of the plate to the jet flow. In other words, the high-frequency response of the plate is independent of the orientation of the plate. This is quite reasonable because turbulence fluctuations are three-dimensional [18] and the associated noise radiated is less directionally dependent. In addition, the low-frequency response of the plate is summarized in Table 1 for further comparison. From Table 1, it can be observed that, for the five x/D locations and the three inclination angles studied, the low frequencies are either 2, 4, 7 and 9 times of 19·5 Hz. That is to say they are all harmonics of 19·5 Hz and are caused by the leapfrogging interaction of ring vortices. In these four multiples, the multiple of 2 and 4 are the dominated ones. However, despite of the same root cause for the forced excitation of the thin plate, the response level is not always the same. In fact, the low-frequency response level of the plate for $\theta = 0$ and 45° is about 5–10 dB greater than that of the 90°. This is quite interesting. It is well known that a ring vortex tends to develop circumferential instabilities [19]. The disturbance caused by this type of an instability is a more effective noise source for a plate installed in parallel to the jet axis. It is not an effective excitation source for a plate installed perpendicular to the jet axis. This is simply because the circumferential instability causes larger disturbance in the direction perpendicular to the jet axis. It should be mentioned that the trend for the Mach number 0·1 case is similar. However, compared to the numerical study of Fenno *et al.* [15], the low-frequency

component of the present study plays a much heavier role in the structural vibration of a thin plate of a similar configuration. It is noted that the Mach number of their study is nearly sonic, much larger than the present one. Whether the difference is due to different Mach numbers needs to be investigated further.

4. CONCLUSIONS

In this study, experiments are conducted to investigate the jet velocity and noise field and the associated structural vibration of a thin aluminum plate at low Mach numbers. Key results are summarized as follows:

1. In the potential core of the turbulent jet, the frequency spectrum exhibits features of low frequency with side band (due to the leap-frog interaction of ring vortices), discrete high frequency and its harmonics (due to shear layer instability) and wide band frequency distribution of low-level random noise. Downstream of the potential core, the flow is characterized by both turbulence fluctuations and low-frequency components.
2. Near the nozzle exit, the noise field is dominated by high-frequency components. The high-frequency components drop out quickly as x/D increases and the low-frequency part of the noise becomes the dominated one.
3. The structural response of a thin plate to the jet is due to two causes. One is a low-frequency forced excitation due to the leap-frog interaction of ring vortices, a directionally dependent mode. The other one is a high-frequency natural response of the plate due to turbulent fluctuations in the jet, a directionally and position-independent mode.

ACKNOWLEDGMENTS

Parts of this work were sponsored by National Science Council, Republic of China, under Contract No. NSC 86-2623-D006-007. This financial support is greatly acknowledged.

REFERENCES

1. H. MARTIN 1977 *Advances in Heat Transfer* **13**, 1–60. Heat and mass transfer between impinging gas jets and solid surface.
2. N. DITTON and C. M. HO 1985 *Journal of Fluid Mechanics* **160**, 235–256. Unsteady separation in a boundary layer produced by an impinging jet.
3. N. RAJARATNAM 1976 *Turbulent Jets*. Amsterdam: Elsevier Scientific Publishing Company.
4. P. J. MORRIS and C. K. W. TAM 1977 *American Institute of Aeronautics and Astronautics paper* 77-1351. Near and far field noise from large-scale instabilities of axisymmetric jets.
5. J. L. STROMBURG, D. K. MCLAUGHLIN and T. R. TROUTT 1979 *American Institute of Aeronautics and Astronautics paper* 79-0593. Flowfield and acoustic properties of a Mach number 0,9 jet at a loe Reynolds number.
6. T. R. TROUTT and D. K. MCLAUGHLIN 1982 *Journal of Fluid Mechanics* **116**, 123–156. Experiments on the flow and acoustic properties of a moderate-Reynolds-number supersonic jet.
7. A. A. GURZHII and V. V. MELESHKO 1996 *Acoustical Physics* **42**, 43–50. Sound emission by a system of vortex rings.
8. A. K. F. M. HUSSAIN 1983 *Physics of Fluids* **26**, 2816–2850. Coherent structures: reality and myth.
9. K. B. M. O. ZEMANM 1985 *Journal of Fluid Mechanics* **152**, 83–111. Far field noise of a subsonic jet under controlled excitation.
10. J. E. BRIDGES and A. K. M. F. HUSSAIN 1987 *Journal of Sound and Vibration* **117**, 289–311. Roles of initial condition and vortex paring in the jet noise.

11. S. B. VERMA and E. RATHAKRISHNAN 1999 *Journal of Sound and Vibration* **226**, 383–396. An experimental study on the noise characteristics of notched circular-slot jets.
12. M. BRASSARD, R.-H. CHEN and L. CHEW 1996 *Journal of Sound and Vibration* **197**, 255–261. An experimental study of underexpanded square jet noise.
13. D. A. BIES, J. M. PICKLES and D. J. J. LECLERCQ 1997 *Journal of Sound and Vibration* **204**, 631–643. Aerodynamic noise generation by a stationary body in a turbulent air stream.
14. M. R. DAVIS and N. H. PAN 1993 *Journal of Sound and Vibration* **167**, 165–181. Noise generated by a turbulent jet interacting with a rigid plate.
15. C. C. FENNO JR , A. BAYLISS and L. MAESTRELLO 1997 *American Institute of Aeronautics and Astronautics Journal* **35**, 219–227. Panel-structure response to acoustic forcing by a nearly sound jet.
16. M. T. ISLAM and M. A. ALI 1997 *American Institute of Aeronautics and Astronautics Journal* **35**, 196–197. Mean velocity and static pressure distribution of a circular jet.
17. D. S. STEINBERG 1988 *Vibration Analysis for Electronic Equipment*. New York: John Wiley & Sons.
18. J. O. HINZE 1975 Turbulence. New York: McGraw-Hill, Inc.
19. D. LIEPMANN and M. GHARIB 1992 *Journal of Fluid Mechanics* **245**, 643–668. The role of streamwise vorticity in the near-field entrainment of round jets.